

# Establishment of the Muscle–Tendon Junction During Thorax Morphogenesis in *Drosophila* Requires the Rho-Kinase

Franco Vega-Macaya,\* Catalina Manieu,\* Mauricio Valdivia,\* Marek Mlodzik,<sup>†</sup> and Patricio Olguín\*<sup>1</sup>

\*Program in Human Genetics, Institute of Biomedical Sciences, Biomedical Neurosciences Institute, Faculty of Medicine, University of Chile, Santiago, Chile 8380453 and <sup>†</sup>Department of Developmental and Regenerative Biology, Icahn School of Medicine at Mount Sinai, New York 10029

ORCID ID: 0000-0002-8847-4969 (P.O.)

**ABSTRACT** The assembly of the musculoskeletal system in *Drosophila* relies on the integration of chemical and mechanical signaling between the developing muscles with ectodermal cells specialized as “tendon cells.” Mechanical tension generated at the junction of flight muscles and tendon cells of the notum epithelium is required for muscle morphogenesis, and is balanced by the epithelium in order to not deform. We report that *Drosophila* Rho kinase (DRok) is necessary in tendon cells to assemble stable myotendinous junctions (MTJ), which are required for muscle morphogenesis and survival. In addition, DRok is required in tendon cells to maintain epithelial shape and cell orientation in the notum, independently of *chascon* (*chas*). Loss of DRok function in tendon cells results in misorientation of tendon cell extensions and abnormal accumulation of Thrombospondin and  $\beta$ PS-integrin, which may cause abnormal myotendinous junction formation and muscle morphogenesis. This role does not depend exclusively on nonmuscular Myosin-II activation (Myo-II), indicating that other DRok targets are key in this process. We propose that DRok function in tendon cells is key to promote the establishment of MTJ attachment and to balance mechanical tension generated at the MTJ by muscle compaction.

**KEYWORDS** myotendinous junction; Rho-kinase; epithelial morphogenesis

**T**HE development of muscle–tendon interaction is a great example of how chemical and mechanical signaling between interacting tissues integrates to regulate cell differentiation and morphogenesis (SCHWEITZER *et al.* 2010; XU *et al.* 2012; WEITKUNAT *et al.* 2014). In *Drosophila*, a great amount of work has been devoted to understanding the mechanisms by which embryonic muscles target and attach to specific epidermal muscle attachment sites (MAS) (FROMMER *et al.* 1996; SUBRAMANIAN *et al.* 2007; WAYBURN and VOLK 2009; GILSOHN and VOLK 2010a, 2010b; ORDAN *et al.* 2015; ORDAN and VOLK 2015), how MAS are specified by patterning signals (Volk and VijayRaghavan 1994; USUI *et al.* 2004), and the role of attachment in MAS differentiation as tendon cells (NABEL-ROSEN

*et al.* 1999, 2002; VOLOHONSKY *et al.* 2007). Moreover, studies of the interaction between the indirect flight muscle (IFM) and the notum epithelium have contributed to unveiling the role of mechanical signaling in muscle and epithelial morphogenesis (OLGUIN *et al.* 2011; WEITKUNAT *et al.* 2014). Nevertheless, the mechanisms by which tendon cells sense chemical and mechanical cues at the developing junction to generate stable muscle–tendon connections and balance mechanical stress is still poorly understood.

Differentiating embryonic and adult tendon cells provide positional cues that direct the targeting of myotube filopodia toward them. Targeting of embryonic muscle toward tendon cells relies on the Slit-Robo system, the leucine-rich tendon specific protein (Lrt), and the matrix proteins Thrombospondin (Tsp) and Slowdown (CHANANA *et al.* 2007; SUBRAMANIAN *et al.* 2007; WAYBURN and VOLK 2009; GILSOHN and VOLK 2010a, 2010b). Attachment initiates with the secretion of extracellular matrix components, including Tsp and laminin, and accumulation of integrins at myotube and tendon membranes (SUBRAMANIAN *et al.* 2007; MAARTENS and BROWN 2015). Subsequently, a few hours later, myofibrillogenesis begins, driving

Copyright © 2016 by the Genetics Society of America  
doi: 10.1534/genetics.116.189548

Manuscript received March 20, 2016; accepted for publication August 16, 2016; published Early Online August 30, 2016.

Supplemental material is available online at [www.genetics.org/lookup/suppl/doi:10.1534/genetics.116.189548/-/DC1](http://www.genetics.org/lookup/suppl/doi:10.1534/genetics.116.189548/-/DC1).

<sup>1</sup>Corresponding author: Program in Human Genetics, Institute of Biomedical Sciences, Biomedical Neurosciences Institute, Faculty of Medicine, University of Chile, Independencia 1027, Santiago, RM 8380453, Chile. E-mail: patricioolguin@med.uchile.cl

myotube compaction, which in turn pulls tendon cells inside the thoracic cavity (METCALFE 1970; OLGUIN *et al.* 2011; WEITKUNAT *et al.* 2014). In response to mechanical tension, tendon cells then extend thin processes enriched in microtubules, F-actin, and Myosin-II (Myo-II) along their apical–basal axis (REEDY and BEALL 1993; OLGUIN *et al.* 2011; WEITKUNAT *et al.* 2014), similar to embryonic tendon cells (SUBRAMANIAN *et al.* 2003; ALVES-SILVA *et al.* 2008). Inhibiting tension buildup either by laser ablation of tendon processes or by genetically compromising muscle–tendon attachment formation, results in strong myofibrillogenesis defects, indicating that mechanical stimuli are required for muscle morphogenesis (WEITKUNAT *et al.* 2014). In addition, disturbing the structure of the actin meshwork of tendon cells, either by loss of function of the actin crosslinker *jbug/Filamin* or *chas* (a *Jbug/Filamin* partner), or interfering with nonmuscle Myo-II, results in cell and tissue deformation (OLGUIN *et al.* 2011). Thus, to establish muscle–tendon interactions and in order not to deform, tendon cells respond to pulling forces by adjusting their adhesive and mechanical properties through strengthening of the myotendinous junction and reorganization of the cytoskeleton.

Rho-kinase is a serine/threonine kinase that regulates cell adhesion, axon growth, planar cell polarity, and cytokinesis, among other cellular processes (WINTER *et al.* 2001; RIENTO and RIDLEY 2003). In both vertebrates and flies, Rho-kinase regulates acto-myosin contractility. Once activated by Rho-GTPase, it phosphorylates the myosin regulatory light chain (MRLC) and the myosin-binding subunit of myosin phosphatase, leading to the activation of nonmuscle Myo-II and the formation of stress fibers and focal adhesion in cultured cells (AMANO *et al.* 1996; KIMURA *et al.* 1996; KAWANO *et al.* 1999). Rho-kinase activation mediated by RhoA is regulated by integrin-based cell-matrix adhesion and requires traction forces mediated by cytoskeletal tension (ROSSMAN *et al.* 2005; SCHILLER 2006; BHADRIRAJU *et al.* 2007). Since Rho-kinase signaling is situated at the interface between mechanical and chemical signaling, we analyze here its role in the development of muscle–tendon interactions and notum epithelium morphogenesis. Flies lacking *Drosophila* Rho kinase (DRok) in the notum epithelium display deformation of the notum epithelium and defects in the targeting of tendon cell processes to the IFMs, which leads to defective myotendinous junction, abnormal muscle morphogenesis, and detachment. In contrast to its role in regulating trichome number (WINTER *et al.* 2001), DRok function in myotendinous junction formation does not rely exclusively on nonmuscle Myo-II, suggesting that other yet unknown DRok targets are crucial for this function.

Our work shows that DRok is required in tendon cells to establish stable connection with the IFMs and to respond to the pulling forces generated by muscle compaction in order to maintain epithelial integrity and polarity.

## Materials and Methods

### Fly strains and genetics

Overexpression studies were performed using the Gal4/UAS system (BRAND and PERRIMON 1993). We used the following

UAS lines: *UAS-DrokiR* (3793 and 104675), *UAS-chasiR* (31766), *UAS-MysiR* (29619), *UAS-SqhiR* (7917) (Vienna *Drosophila* RNAi Center), *UAS-CD8-ChRFP* (Bloomington *Drosophila* Stock Center; BDSC), *UAS-sqh[E20E21]* (Winter *et al.* 2001), and *UAS-DFos<sup>N Ala</sup>* (CIAPPONI *et al.* 2001). We also used the following Gal4 lines: *Pnr-Gal4* and *Sr-Gal4* (BDSC). Mitotic *chas<sup>1</sup>* clones were generated using the FLP/FRT (XU and RUBIN 1993) marked with yellow. For *chas* rescue with *DrokiR*, and for *Drok<sup>2</sup>* (BDSC) clonal analysis we used the mosaic analysis with a repressible cell marker (MARCM) system (LEE and LUO 1999). *MHC-TauGFP* was used to visualize muscle fibers (CHEN and OLSON 2001). All phenotypes were analyzed at 25° unless stated otherwise.

### Immunohistochemistry and imaging

Primary antibodies were  $\beta$ -integrin (1/20, Hybridoma bank, DSHB), Tsp (1/100, courtesy of T. Volk, Department of Molecular Genetics, Weizmann Institute of Science, Rehovot, Israel), anti-phospho-sqh (1/500, courtesy of Robert E. Ward IV, Department of Molecular Biosciences, University of Kansas), and anti-GFP (1/1000, Molecular Probes, Eugene, OR). Secondary antibodies were from Jackson Immunological Laboratories (1/200), F-actin was stained with Rhodamine-phalloidin (1/500, Molecular Probes), and nuclei were stained with DAPI (1/1000, Molecular Probes). Dissected muscle preparations were obtained from staged pupae. Pupae of the desired age were removed from the pupal case, pinned down on Sylgard plates, and dissected in cold PBS. The fixation was carried out with 4% paraformaldehyde in PBS (PFA) for 40 min at room temperature. Following washes in PBS containing 0.3% Triton X-100, the tissue was incubated with antibodies diluted in 0.3% Triton X-100 and 10% bovine serum albumin as blocking reagent. Stained samples were mounted in Vectashield (Vector Laboratories, Burlingame, CA), confocal images were captured using a Carl Zeiss LSM 700 confocal microscope (Thornwood, NY). Agarose sectioning of pupae using a vibratome was performed according to (WEITKUNAT and SCHNORRER 2014). For scanning electron microscopy adult flies were fixed in ethanol 95%, dried to critical point, sputter coated, and imaged with a Hitachi S-2600H scanning electron microscope. Pictures of adults were taken in an Infinity 1 digital camera and processed using Adobe Photoshop CS5 Extended.

### Live imaging of pupal notum

White pupae of the indicated genotype were collected, aged at 25°, and mounted as described (BELLAICHE *et al.* 2001). Images were acquired using a Leica TCS LSI confocal microscope. Fifteen confocal planes (0.2  $\mu$ m depth) of nota expressing *UAS-CD8-RFP* under the control of *srGal4* and *MHC-TauGFP* were taken at 20 min intervals for 5 hr. Filopodial angles of tendon cells and myotubes with respect to the lateral posterior end of the *sr* domain were measured in three independent movies by using ImageJ (National Institutes of Health), analyzed with Prism 4 software, shown as Rose diagrams (Rose 2.1.0, <http://mypage.iu.edu/~7Etthomps/programs/home.htm>), and analyzed with Student's *t*-test. *P* values were

calculated using Student's *t*-test. A *P* value < 0.01 was considered to show a significant difference. For the filopodia angle profile, Welch's correction was used assuming similar means, but differences in SD.

### Data availability

The authors state that all data necessary for confirming the conclusions presented in the article are represented fully within the article.

## Results and Discussion

### *DRok is required for notum epithelium morphogenesis and polarity*

We have shown previously that nonmuscle Myo-II and *chas* are required in tendon cells to maintain notum epithelium shape and polarity in response to the pulling forces generated by dorsal longitudinal muscles (DLMs) compaction (OLGUIN *et al.* 2011). Since DRok is the main regulator of Myo-II activity through phosphorylation of MRLC, and its activity is regulated by mechanical tension and integrin signaling in other models (ROSSMAN *et al.* 2005; SCHILLER 2006; BHADRIRAJU *et al.* 2007), we tested whether it plays a role in the mechanoresponse of tendon cells to mechanical forces generated by interactions with IFMs. To interfere with *Drok* expression we used two nonoverlapping double-stranded RNAs (dsRNAs), *DrokiR* and *DrokiR2* (Supplemental Material, Figure S1). The expression of either dsRNAi targeting *Drok* under the control of the *pnrGal4* driver results in mild notum closure defects at the midline (Figure 1, cf. C and 1A, and Figure S1) and in multiple hairs per cell, as has been described in the wing epithelium lacking *fz* or *Drok* (Figure 1C') (WINTER *et al.* 2001). Since both dsRNAs display similar phenotypes, we used *DrokiR* for subsequent experiments (Figure S1). *DrokiR*-expressing cells located at the most lateral region of the *pnr* expression domain display bristles and trichomes pointing toward the midline, similar to *chas* knockdown phenotypes (Figure 1, cf. C'' and B'', arrowheads) (OLGUIN *et al.* 2011). At this lateral domain (Figure 1, A–C, indicated with yellow squares), animals expressing either *chasiR* or *fziR* in combination with *DrokiR* displayed enhanced trichome orientation phenotypes (Figure 1D'' and Figure S2). In addition, scanning electron microscope (SEM) images reveal small invaginations of the epithelium toward the thoracic cavity (Figure 1D'' and Figure S2), suggesting that *Drok* is required in tendon cells to maintain epithelial integrity and cellular orientation through the balance of the pulling forces generated by muscle compaction. Epithelial cell deformation is consistent with the deformation of *Drok*<sup>2</sup> oocytes due to detachment of the apical membrane of follicular cells during oogenesis. This effect has been attributed to disorganization of cortical actin networks due to diminished levels of moesin and Myo-II (VERDIER *et al.* 2006). DRok might play a similar role organizing the apical actin network through regulation of these proteins.

Unexpectedly, *Drok* knockdown rescues both the indentation and the orientation defects associated with *chas* knockdown in the anterior and central region of the *pnr* domain, respectively (Figure 1, D and D'). Since the expression of a dominant negative of Zipper, the *Drosophila* Myo-II heavy chain, in a *chas* background enhances *chas* phenotypes (OLGUIN *et al.* 2011), we presume that other targets of DRok are involved in this phenotype.

*Drok* notum closure phenotypes are reminiscent of defective heminota migration toward the midline and/or fusion, a process that is finished by 6.5 hr after puparium formation (hAPF), previous to the early stages of muscle–tendon attachment (ZEITLINGER and BOHMANN 1999; MARTIN-BLANCO *et al.* 2000). Heminota fusion defects associated with loss of Jnk result in bristle orientation toward the lateral side (with respect to the midline), similar to *DrokiR* expression, although in a much stronger manner (MARTIN-BLANCO *et al.* 2000). Based on these data, we reasoned that defective heminota migration could indirectly revert *chas* cell orientation phenotypes. Knockdown of the Jnk pathway in combination with *chas* knockdown only partially suppresses cell orientation defects associated with *chas* loss of function, indicating that polarity defects associated with heminota migration or fusion are not sufficient to revert the *chas* phenotype (not shown). To avoid heminota migration defects, we expressed *DrokiR* in *chas*<sup>1</sup> mitotic clones using the MARCM system (LEE and LUO 2001). Cells expressing *DrokiR* did not affect heminotum migration, and MARCM clones located at lateral and central positions of the notum reverted their *chas*<sup>1</sup> orientation phenotypes (Figure S3). Taken together, these data show that *Drok* knockdown rescues *chas* associated cell orientation defects, independently of its role in dorsal thorax closure.

### *DRok is required in tendon cells for muscle survival independently of Myo-II*

Since Myo-II knockdown and *chas* cell orientation phenotypes depend on the interaction of the notum epithelium with the underlying IFMs (OLGUIN *et al.* 2011), we reasoned that *Drok* could be required in tendon cells for muscle development or myotendinous junction formation in addition to its role in epithelial morphogenesis. Therefore, diminished DRok activity in tendons should reduce or abrogate pulling forces generated by muscle compaction. Sagittal sections of adults expressing *DrokiR* under *pnrGal4* appears to lack dorsal longitudinal IFMs (Figure 1C''), suggesting that *Drok* is required in tendon cells for muscle development or maintenance. Since MRLC, encoded by the spaghetti squash (*sqh*) gene, is the main effector of DRok, we asked whether its phosphorylation is altered in tendon cells lacking *Drok*. *Drok*<sup>2</sup> mutant cells displayed reduced levels of phosphorylated Sqh (Sqh-P) from the apical level through tendon cells processes (Figure 2, A and B') (ZHANG and WARD 2011). At the myotendinous junction the reduction of Sqh-P staining appears weaker than at the other levels, which can be due to expression of *Drok* at the muscle cells. Interestingly, myotubes attached to mutant tendons are shorter displaying irregular anterior edge



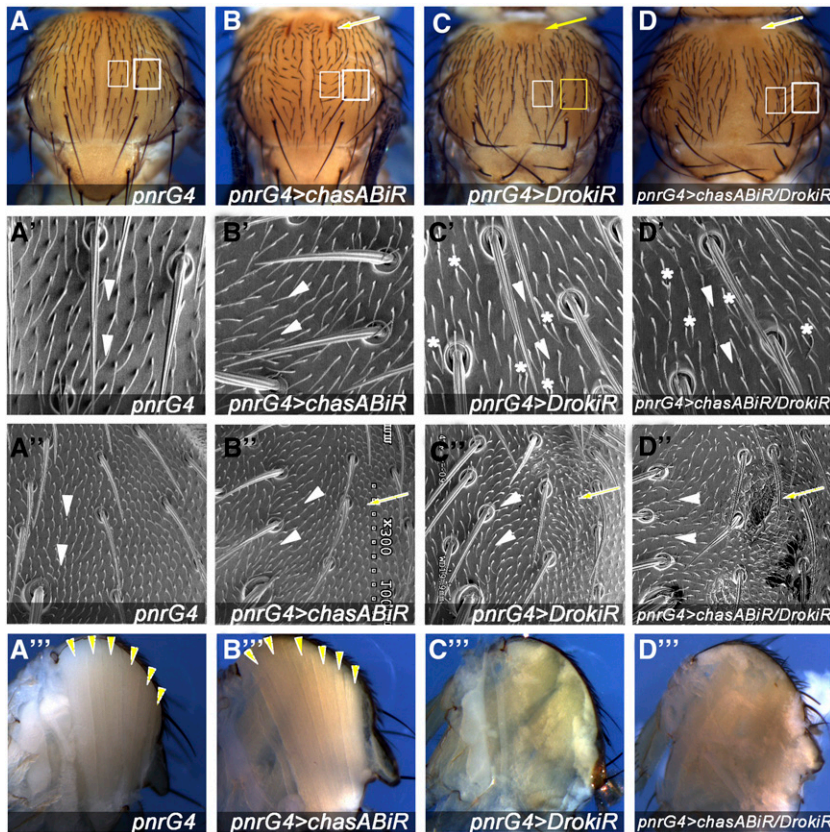


**Figure 1** *Drok* is required for notum morphogenesis. (A–D) Adult notum of flies expressing the indicated *dsRNAi* under the control of *pnrGal4*. Arrowheads indicate indentations of the notum epithelium. (A–D) White square marks central notum region analyzed in (A'–D'); yellow square indicates lateral regions analyzed in (A''–D''). (A'–D'') SEM images of adult flies showing orientation of trichomes (arrowheads), invaginations of the notum epithelium (arrows) and multiple hairs per cell (asterisks). (A''–D'') Sagittal sections of adult thorax, showing dorsal longitudinal muscles (DLMs) (arrowheads). Note that dorsal longitudinal IFMs appears to be reduced or absent (C'') and (D'').

compared with its contralateral counterparts (Figure 2, cf. C and D, and C' and D'). Moreover, other myotubes detach from the epithelium, supporting our previous observations in adults using *DrokiR* (Figure 2, D and D'). To answer whether inhibition of Myo-II activity results in muscle degeneration, we expressed a *dsRNAi* targeting (*sqh*), at different larval developmental stages using *pnrGal4* and *tubGal80ts* to bypass its cytokinesis role (MURTHY and WADSWORTH 2005). Expression of *sqhiR* starting at second instar larval stage resulted in dorsal thorax closure defects and muscle degeneration, suggesting that the role of *Drok* in muscle development may depend on Myo-II activity, although this effect could be an indirect consequence of abnormal thorax closure (Figure S4). In addition, the activation of *sqhiR* expression at early third instar larval stage results in anterior invaginations of the notum epithelium and in cell orientation defects without affecting muscle integrity, confirming Myo-II role tendon cell adaptation to mechanical stress (Figure S4). Strikingly, the expression of a constitutively active form of MRLC (SqhE20E21) in the epithelium did not rescue the muscle degeneration phenotype associated with *Drok* loss of function (Figure 3, cf. I and H), but it did partially rescue notum dorsal closure and multiple hairs per cell phenotypes (Figure 3, A–F), as was shown previously in the wing epithelium (WINTER *et al.* 2001), supporting the idea that other *Drok* targets are required in tendon cells for muscle survival.

To investigate at which stage of development IFMs degenerate in *Drok* knockdown conditions, we monitored muscle development in animals expressing tauGFP under the control of the muscle myosin heavy chain promoter (MHC-tauGFP) (CHEN and OLSON 2001) (Figure 4). Animals expressing *DrokiR* under *srGal4* (*srGal4 > DrokiR*) displayed shortened muscles compared to control animals expressing only the *srGal4* driver at 47 hAPF (Figure 4, cf. A and B). At 55 hAPF a gap develops between DLMs dorsal and ventral fibers, which display reduced size and irregular anterior and posterior edges, suggesting irregular attachments to the epithelium (Figure 4B''). Sagittal sections of 98 hAPF nota reveal a gap between dorsal and ventral myotubes, indicating the lack of DLMs fibers (Figure 4, cf. H and G). Finally, inspection of remaining DLMs in *srGal4 > DrokiR* animals reveals mildly irregular myofibrils (Figure 4H'). To confirm our results we expressed *DrokiR* driven by *pnrGal4* (*pnrGal4 > DrokiR*), since it resulted in stronger phenotypes than with *srGal4*. Like *srGal4 > DrokiR*, these animals displayed enhanced shortening of DLMs (Figure 4, cf. C and C' with E and E'), which is already significant at 24 hAPF, although with similar width (Figure S5). In contrast to *srGal4 > DrokiR*, the overshortening of DLMs increases through development and correlates with irregular attachment to tendon cell processes (Figure 4, D' and F'). Finally, *pnrGal4 > DrokiR* animals display completely degenerated muscles, which is confirmed by sagittal sections of 76 hAPF nota (Figure 4, J and J'). We did not find differences in the number

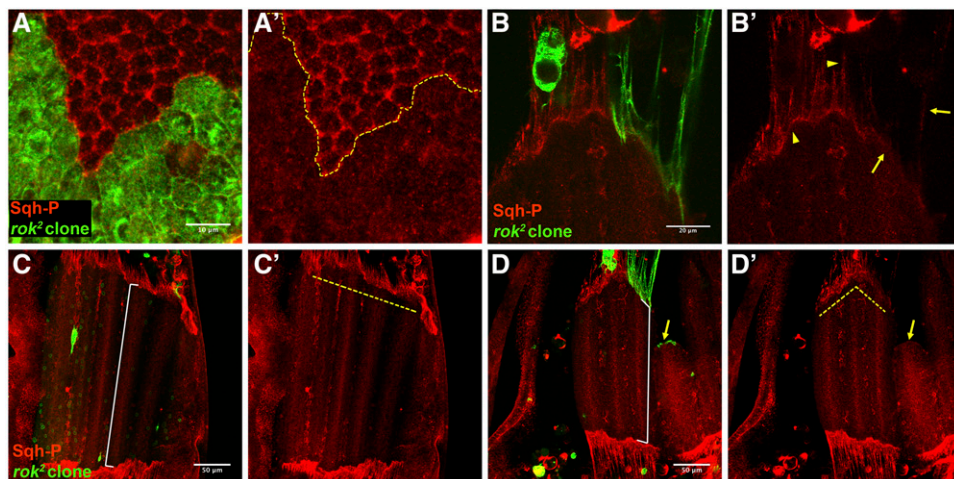


**Figure 2** *Drok* loss of function in tendon cells results in diminished Sqh phosphorylation and disturbs muscle morphogenesis. (A, A') *Drok*<sup>2</sup> mutant clone of notum epithelial cells (27 hAPF) marked with CD8-GFP displays diminished levels of monophosphorylated Sqh (Sqh-P) at the apical side. (B, B') *Drok*<sup>2</sup> mutant tendon cell processes and myotendinous junction display diminished levels of Sqh-P (arrows), cf. wild type tendon extension and myotendinous junction (arrowheads). (C–D') Confocal projections of DLMs at 27 hAPF of an animal carrying a *Drok*<sup>2</sup> clone at the right side (D, D'). DLMs attached to wild type tendon cells display a regular anterior edge (dashed yellow line) (C'), while

DLMs attached to a group of *Drok*<sup>2</sup> tendon cell processes display irregular anterior edge (dashed yellow line) (D') and display detachment of the epithelia (arrow). Note that myotubes attached to *Drok*<sup>2</sup> tendon processes are shorter than the contra lateral muscles, cf. white guide of (C) and (D).

of nuclei between IFMs attached to either wild-type or *DrokiR*-expressing tendon cells at 24 hAPF using both drivers (Figure S5). Thus, we conclude that muscle morphological defects and degeneration occurs after myoblast fusion and muscle–tendon connection.

Based on these results we propose that a muscle overcompaction and deformation phenotypes, along with the loss of myotube ability to extend back after compaction (Figure 4) are due to irregular attachment and unbalanced pulling forces by tendon cells. These phenotypes are consistent with the morphology of muscles observed in *Drok*<sup>2</sup> mosaic animals, where myotubes attached to mutant tendon cells are shorter than myotubes attached to wild type cells, and even detach from mutant tendon cells (Figure 2). Since pulling forces would not be distributed homogeneously along the anterior and posterior edges of myotubes at the myotendinous junction, deformation of muscle fibers may result. This idea is in agreement with observations from Frank Schnorrer's group, who has shown elegantly that pulling forces generated by muscle compaction at myotendinous junction are required for correct myofibrillogenesis and muscle morphogenesis (WEITKUNAT *et al.* 2014).

#### ***Drok* is required in tendon cells for myotendinous junction formation**

It has been shown previously that, during embryogenesis, the correct assembly of the myotendinous junction depends on the coordinated accumulation of  $\alpha$ PS2- $\beta$ PS integrin heterodimers at the muscle leading edge, with the deposition of the tendon-derived extracellular matrix (ECM) protein Tsp (SUBRAMANIAN *et al.* 2007; GILSOHN and VOLK 2010b). Tsp mediates the binding of  $\alpha$ PS2- $\beta$ PS heterodimers to the ECM during myotendinous junction formation, and its premature deposition results in accumulation of  $\alpha$ PS2- $\beta$ PS and irregular architecture of the myotendinous junction (GILSOHN and VOLK 2010b). We observed that *Drok* loss of function

resulted in normal accumulation of Tsp and irregular accumulation of  $\beta$ PS integrin at the attachment region at 24 hAPF (Figure 5, cf. D with D'). At 32 hAPF Tsp and  $\beta$ PS integrin accumulates along the tendon processes (Figure 5H'), with Tsp displaying a spotty pattern (Figure 5, G and G'). Strikingly, F-actin staining of notum epithelia expressing *DrokiR*, revealed disorganized tendon extensions that appeared to interact with each other or group into bundles (Figure 5, F and F'). Similarly, phalloidin staining of *Drok*<sup>2</sup> tendon cell processes reveals disorganized filaments compared to wild-type cells, which display more parallel arrangement of tendon processes (Figure 5K, cf. left and right side). On the other hand, integrin staining accumulates mildly in a spotty fashion on *Drok*<sup>2</sup> clone territory, although not as clearly as in the *DrokiR* condition (Figure 5L). This phenotype is reminiscent of animals with diminished expression of *kon-tiki* (*kon*) in embryonic myotubes (SCHNORRER *et al.* 2007). *Kon* is a single pass transmembrane protein of the neurexin family that is required in ventrolateral embryonic myotubes to recognize its tendon targets and generate stable junctions (SCHNORRER *et al.* 2007). How can loss of function of either *Drok* at tendons, or *Kon* at myotubes, generate such similar phenotypes? During development of the adult myotendinous junction, *Kon* appears to be required for the accumulation of  $\beta$ PS integrin at the tips of myotubes (WEITKUNAT *et al.* 2014). Therefore its loss of function results in defective recognition between tendon and myotubes. Accordingly, abnormal deposition of Tsp by tendon cells lacking *Drok* might lead to defective recognition by myotube  $\alpha$ PS2- $\beta$ PS integrin receptors and abnormal myotendinous junction formation.

#### ***Drok* regulates tendon extension orientation and shape**

Since *Kon* and *Drok* display similar phenotypes during the myotube compaction stage, we reasoned that junction



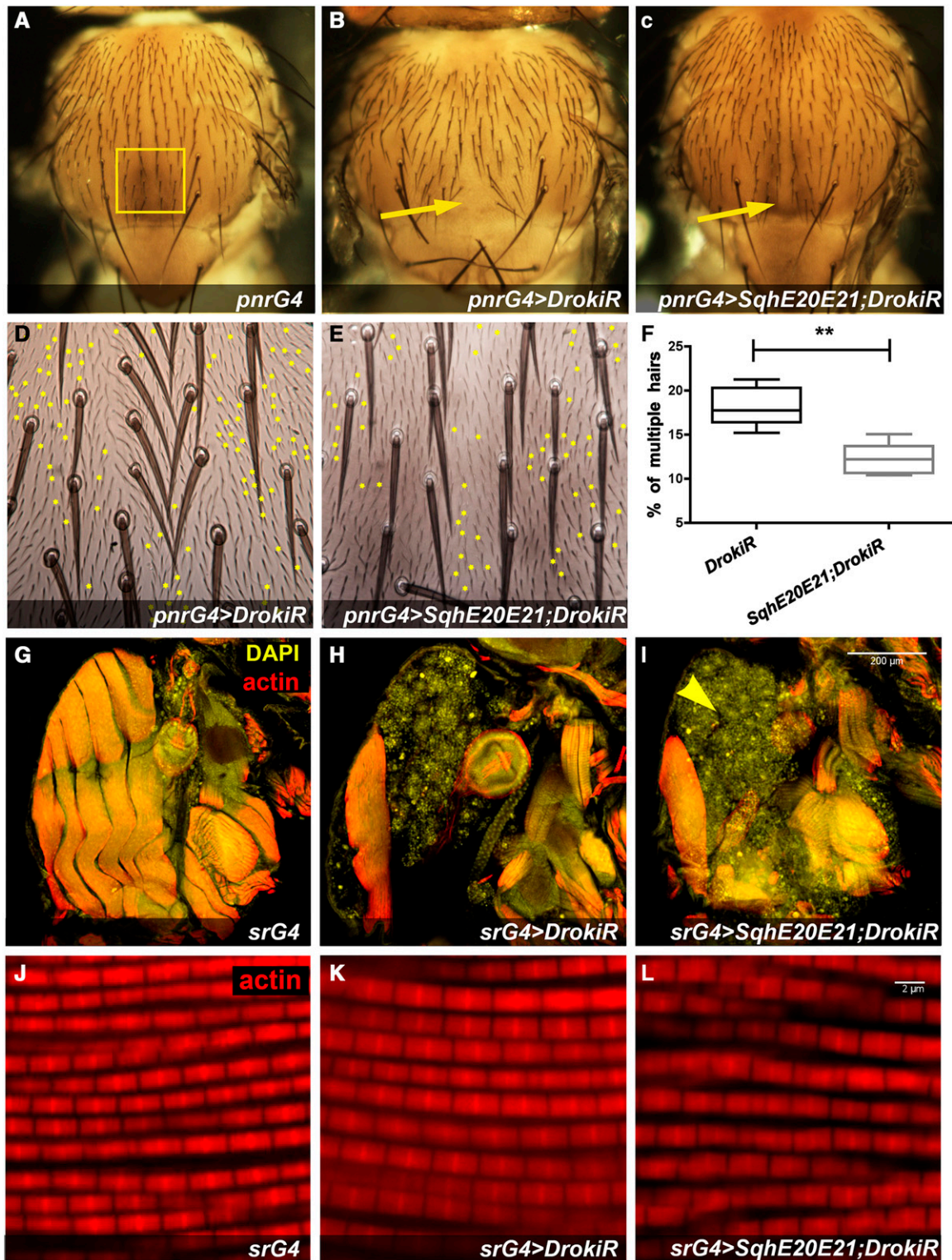


**Figure 3** *Drok* requirement for muscle survival does not depend exclusively on Myo-II. (A–C) Expression of *SqhE20E21* driven by *pnrG4* partially rescues dorsal thorax closure, cf. (B) and (C) (20% penetrance  $n = 20$ ) (arrows); and multiple hairs per cell, indicated with yellow asterisks, cf. (D) with (E),  $P = 0.0022$  (F), associated with *DrokiR* expression. Regions analyzed in (D) and (E) correspond to the region indicated with a square in (A). (G–I) Sagittal sections of thorax stained with phalloidin and DAPI. Expression of *SqhE20E21* using *srG4* driver does not rescue muscle degeneration associated to expression of *DrokiR* (arrowhead). (J–L) Detail showing myofibrils. Note that remaining muscle fibers are normal, cf. (K) and (L) with (J). (G–I) Bar, 200  $\mu\text{m}$ . (J–L) Bar, 2  $\mu\text{m}$ . Asterisks in (F) indicate significance  $P = 0.0022$ .

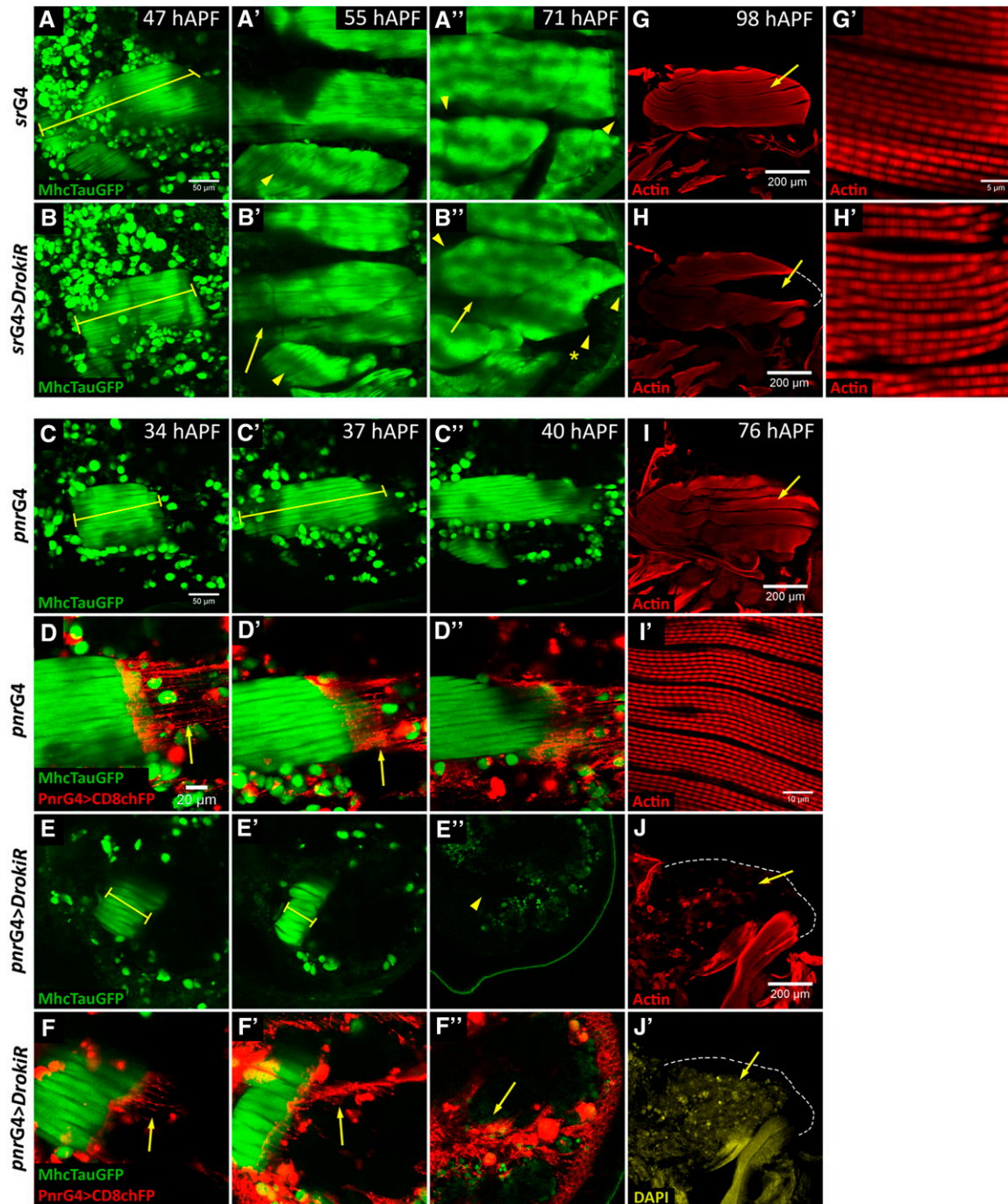


**Figure 4** *Drok* is required in tendon cells for muscle morphogenesis. (A–F’’) Time lapse of DLMs development of flies expressing Tau-GFP under the control of MHC. Genotypes are as indicated to the left. (A, B) Note that developing DLMs remain short in flies expressing *DrokiR* under the control of *srGal4* at 31hAPF, cf. (A) with (B) (rulers). (B’) At 55 hAPF a gap between dorsal and ventral myotubes is evident (arrow), cf. (B). Note that dorso-ventral muscle is smaller than the control, cf. (B) with (B’). (B’’) At 71 hAPF lack DLMs are smaller than the control displaying abnormal shape at the anterior and posterior edges (arrowheads), cf. (A’). Note that anterior dorsoventral muscle is missing (B’’) (asterisk) cf. (B). (C, E’) Overshortening of DLMs of flies expressing *DrokiR* under the control of *pnrGal4*. Note that overshortening increases from 34 to 37 hAPF (E, E’), cf. (C, C’). (E’’) At 40 hAPF DLMs are absent, cf. (C, C’). (D, D’’, F, F’’) Details of (C, C’, E, E’’) showing a confocal projection of the most dorsal tendon processes marked with CD8RFP. Note that tendon processes are irregularly attached to DLMs (arrows). (G–J’) Sagittal sections of 98 hAPF thorax stained with phalloidin (G–J) and DAPI (J’). (H) Gap generated between dorsal and ventral group of DLMs, cf. (G). (H’) Remaining myofibers appear mildly disorganized. (J) Absence of DLMs at 76 hAPF in animals expressing *DrokiR*.

and muscle phenotypes are a consequence of defects that occur at earlier stages of myotendinous junction establishment. We monitored attachment initiation using time

lapse confocal microscopy of flies expressing *MHC-tau-GFP* and *CD8-RFP* driven by *srGal4*, to examine myotube and tendon processes, respectively (Figure 6, Figure S6, File S1, and



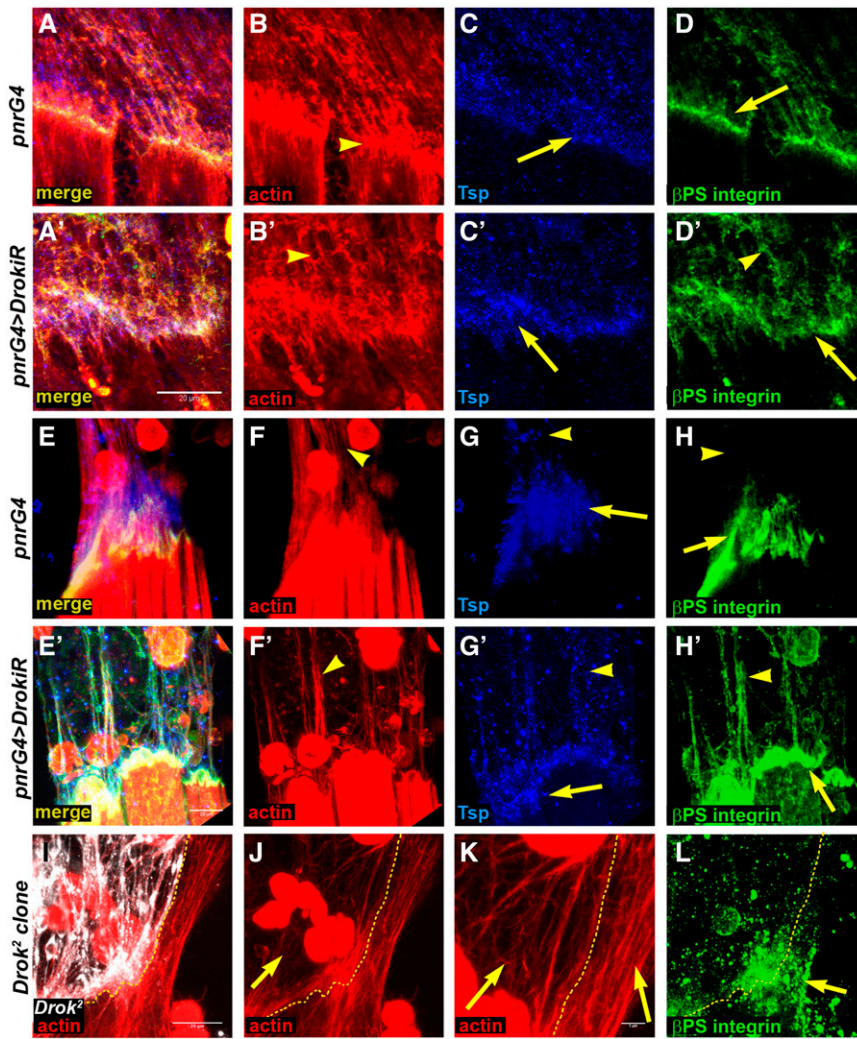


**Figure 5** *Drok* is required for myotendinous junction formation. Confocal projections of myotendinous junctions at 24 hAPF (A–D') and 32 hAPF (E–H') stained with phalloidin/F-actin (B, B', F, F', J, K), Tsp (C, C', G, G') and βPS-integrin (D, D', H, H', L). Genotypes as indicated on left. (B, B', F, F', J, K) Tendon cells extensions arrange irregularly: cf. (B) and (B'), (F) and (F'), and *Drok*<sup>2</sup> clones [I, J, K (detail)] (arrows). Tsp and βPS-integrin accumulate irregularly in tendon cell extensions (arrowheads) and myotube edge (arrows), cf. (C') and (C); (D') and (D); (G') and (G); (H') and (H); and mitotic clones (L). Note that at 24 hAPF, at the myotendinous junction, the abnormal accumulation of Tsp and integrin is not as aberrant as at 32 hAPF. Bar, 20 μm for all images and 5 μm in (K).

File S2). Tendon extensions of cells expressing *DrokiR* appeared disorganized and to cluster from 13 to 18 hAPF (Figure 6, D and D', H and H'). Measurements of the angles formed between tendon processes and the lateral–posterior edge of the *stripe* domain (Figure 6, I and J) showed that *DrokiR* SD of angle measurements doubled the wild type value at 13 hAPF ( $P < 0.0001$ ) and tripled it by 18 hAPF ( $P < 0.0001$ ) (Figure 6K). Interestingly, the SD increased significantly during that time in *DrokiR* expressing animals ( $P = 0.0042$ ) in contrast to wild type, which maintained a similar distribution and average angle values. Distribution of angle measurements of myotube extension of *DrokiR* was wider than controls at 13 hAPF ( $P < 0.0001$ ), but did not show significant differences at 18 hAPF (Figure S6). Taken together, these results indicate that DRok is required in tendon cells for orientation of tendon extension during attachment initiation.

### Conclusions

The RhoA-ROCK pathway plays a key role in coordinating mechanical and chemical signaling in a variety of

processes, including human mesenchymal stem cell differentiation into tendon/ligament-like lineages (RIENTO and RIDLEY 2003; XU *et al.* 2012). We propose that coordination between “outside-in and inside-out mechanical signaling” called mechano-reciprocity, might play a fundamental role in tendon cells for myotendinous junction formation. In our model, *Drok* is pivotal for mechano-reciprocity at the myotendinous junction (Figure 6, L and M). Tendon cells with diminished levels of *Drok* would not be able to respond to mechanical signaling from ECM (outside-in) leading to production of unstable cellular extensions with a wider range of orientations and as a consequence, abnormal secretion (inside-out) of ECM proteins that are required for myotube filopodia attachment, such as Tsp (13–18 hAPF, Figure 6, cf. M and L). Irregular and unstable muscle tendon attachments (Figure 6M, 32 hAPF) result in muscle morphogenesis defects, detachment, and death (Figure 6M, 35+ hAPF).

In summary we have shown that *Drok* is not only required for epithelial morphogenesis and polarity, but importantly also for myotendinous junction formation and



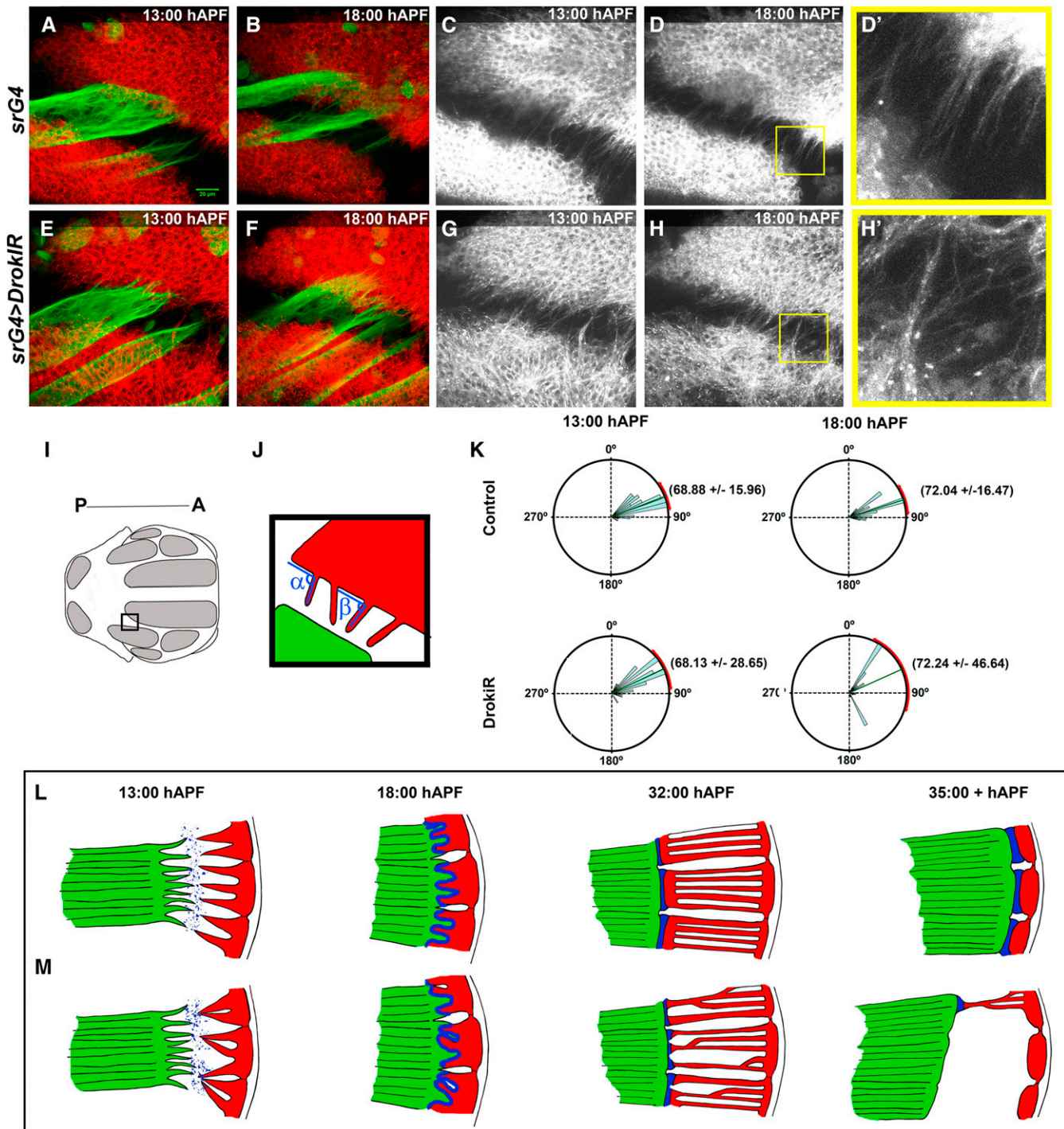


**Figure 6** *Drok* regulates tendon processes orientation and morphology. (A–H) Time points of time-lapse confocal microscopy movies taken from 13 to 18 hAPF of flies expressing MHC-TauGFP and CD8-RFP driven by *srGal4*. (D' and H') Details of (D and H) with a magnification of 3X. (I) Thorax region imaged, posterior is to the left and anterior to the right. (J) Method to measure the angles formed between tendon processes and the lateral-posterior edge of the *sr* domain. (K) Quantification of tendon extensions angles ( $P < 0.0001$ ). (L, M) Scheme of myotendinous junction formation under normal (L) and *Drok* loss of function (M) conditions. Tendon cells (red) with *Drok* loss of function display irregular morphology and orientation during attachment initiation, abnormal secretion of matrix proteins (blue), failure to attach uniformly to myotubes (green), and detachment during muscle compaction.

subsequently for muscle development. Our genetic and cellular analyses suggest that DRok is required at different cellular levels, and its role in myotendinous junction

formation does not depend exclusively on Myo-II activation, indicating that other DRok targets are key in this process.

## Acknowledgments

We thank Alvaro Glavic, Jimena Sierralta, Kenneth Prehoda, Daniel Kiehart, Robert E. Ward IV, and Talila Volk, Berkeley *Drosophila* Genome Project, Vienna *Drosophila* RNAi Stock Center, and the Bloomington Center for flies and reagents; Angélica Figueroa, Fernando Vergara, Paola Sepúlveda, Inés Negrete, and Noemi Candia for technical support; and Ursula Weber for advice and discussion. This work was supported by National Institutes of Health grant GM-62917 to M.M., FONDECYT no. 112053 and Anillo ACT-1401 grants, and Program U-Apoya (University of Chile) to P.O. C.M. is a recipient of a fellowship for graduate students from Consejo Nacional de Ciencia y Tecnología.

## Literature Cited

- Alves-Silva, J., I. Hahn, O. Huber, M. Mende, A. Reissaus *et al.*, 2008 Prominent actin fiber arrays in *Drosophila* tendon cells represent architectural elements different from stress fibers. *Mol. Biol. Cell* 19: 4287–4297.
- Amano, M., M. Ito, K. Kimura, Y. Fukata, K. Chihara *et al.*, 1996 Phosphorylation and activation of myosin by Rho-associated kinase (Rho-kinase). *J. Biol. Chem.* 271: 20246–20249.
- Bellaiche, Y., M. Gho, J. A. Kaltschmidt, A. H. Brand, and F. Schweisguth, 2001 Frizzled regulates localization of cell-fate determinants and mitotic spindle rotation during asymmetric cell division. *Nat. Cell Biol.* 3: 50–57.
- Bhadriraju, K., M. Yang, S. Alom Ruiz, D. Pirone, J. Tan *et al.*, 2007 Activation of ROCK by RhoA is regulated by cell adhesion, shape, and cytoskeletal tension. *Exp. Cell Res.* 313: 3616–3623.
- Brand, A. H., and N. Perrimon, 1993 Targeted gene expression as a means of altering cell fates and generating dominant phenotypes. *Development* 118: 401–415.
- Chanana, B., R. Graf, T. Koledachkina, R. Pflanz, and G. Vorbruggen, 2007 AlphaPS2 integrin-mediated muscle attachment in *Drosophila* requires the ECM protein Thrombospondin. *Mech. Dev.* 124: 463–475.
- Chen, E. H., and E. N. Olson, 2001 Antisocial, an intracellular adaptor protein, is required for myoblast fusion in *Drosophila*. *Dev. Cell* 1: 705–715.
- Ciapponi, L., D. B. Jackson, M. Mlodzik, and D. Bohmann, 2001 *Drosophila* Fos mediates ERK and JNK signals via distinct phosphorylation sites. *Genes Dev.* 15: 1540–1553.
- Frommer, G., G. Vorbruggen, G. Pasca, H. Jackle, and T. Volk, 1996 Epidermal *egr*-like zinc finger protein of *Drosophila* participates in myotube guidance. *EMBO J.* 15: 1642–1649.
- Gilsohn, E., and T. Volk, 2010a Fine tuning cellular recognition: the function of the leucine rich repeat (LRR) trans-membrane protein, LRT, in muscle targeting to tendon cells. *Cell Adhes. Migr.* 4: 368–371.
- Gilsohn, E., and T. Volk, 2010b Slowdown promotes muscle integrity by modulating integrin-mediated adhesion at the myotendinous junction. *Development* 137: 785–794.
- Kawano, Y., Y. Fukata, N. Oshiro, M. Amano, T. Nakamura *et al.*, 1999 Phosphorylation of myosin-binding subunit (MBS) of myosin phosphatase by Rho-kinase in vivo. *J. Cell Biol.* 147: 1023–1038.
- Kimura, K., M. Ito, M. Amano, K. Chihara, Y. Fukata *et al.*, 1996 Regulation of myosin phosphatase by Rho and Rho-associated kinase (Rho-kinase). *Science* 273: 245–248.
- Lee, T., and L. Luo, 1999 Mosaic analysis with a repressible cell marker for studies of gene function in neuronal morphogenesis. *Neuron* 22: 451–461.
- Lee, T., and L. Luo, 2001 Mosaic analysis with a repressible cell marker (MARCM) for *Drosophila* neural development. *Trends Neurosci.* 24: 251–254.
- Maartens, A. P., and N. H. Brown, 2015 The many faces of cell adhesion during *Drosophila* muscle development. *Dev. Biol.* 401: 62–74.
- Martin-Blanco, E., J. C. Pastor-Pareja, and A. Garcia-Bellido, 2000 JNK and decapentaplegic signaling control adhesiveness and cytoskeleton dynamics during thorax closure in *Drosophila*. *Proc. Natl. Acad. Sci. USA* 97: 7888–7893.
- Metcalfe, J. A., 1970 Developmental genetics of thoracic abnormalities of dumpy mutants of *Drosophila melanogaster*. *Genetics* 65: 627–654.
- Murthy, K., and P. Wadsworth, 2005 Myosin-II-dependent localization and dynamics of F-actin during cytokinesis. *Curr. Biol.* 15: 724–731.
- Nabel-Rosen, H., N. Dorevitch, A. Reuveny, and T. Volk, 1999 The balance between two isoforms of the *Drosophila* RNA-binding protein how controls tendon cell differentiation. *Mol. Cell* 4: 573–584.
- Nabel-Rosen, H., G. Volohonsky, A. Reuveny, R. Zaidel-Bar, and T. Volk, 2002 Two isoforms of the *Drosophila* RNA binding protein, how, act in opposing directions to regulate tendon cell differentiation. *Dev. Cell* 2: 183–193.
- Olguin, P., A. Glavic, and M. Mlodzik, 2011 Intertissue mechanical stress affects frizzled-mediated planar cell polarity in the *Drosophila* notum epidermis. *Curr. Biol.* 21: 236–242.
- Ordan, E., and T. Volk, 2015 A non-signaling role of Robo2 in tendons is essential for Slit processing and muscle patterning. *Development* 142: 3512–3518.
- Ordan, E., M. Brankatschk, B. Dickson, F. Schnorrer, and T. Volk, 2015 Slit cleavage is essential for producing an active, stable, non-diffusible short-range signal that guides muscle migration. *Development* 142: 1431–1436.
- Reedy, M. C., and C. Beall, 1993 Ultrastructure of developing flight muscle in *Drosophila*. II. Formation of the myotendon junction. *Dev. Biol.* 160: 466–479.
- Riento, K., and A. J. Ridley, 2003 Rocks: multifunctional kinases in cell behaviour. *Nat. Rev. Mol. Cell Biol.* 4: 446–456.
- Rossman, K. L., C. J. Der, and J. Sondek, 2005 GEF means go: turning on RHO GTPases with guanine nucleotide-exchange factors. *Nat. Rev. Mol. Cell Biol.* 6: 167–180.
- Schiller, M. R., 2006 Coupling receptor tyrosine kinases to Rho GTPases—GEFs what's the link. *Cell. Signal.* 18: 1834–1843.
- Schnorrer, F., I. Kalchauer, and B. J. Dickson, 2007 The trans-membrane protein Kon-tiki couples to Dgrip to mediate myotube targeting in *Drosophila*. *Dev. Cell* 12: 751–766.
- Schweitzer, R., E. Zelzer, and T. Volk, 2010 Connecting muscles to tendons: tendons and musculoskeletal development in flies and vertebrates. *Development* 137: 2807–2817.
- Subramanian, A., A. Prokop, M. Yamamoto, K. Sugimura, T. Uemura *et al.*, 2003 Shortstop recruits EB1/APC1 and promotes microtubule assembly at the muscle-tendon junction. *Curr. Biol.* 13: 1086–1095.
- Subramanian, A., B. Wayburn, T. Bunch, and T. Volk, 2007 Thrombospondin-mediated adhesion is essential for the formation of the myotendinous junction in *Drosophila*. *Development* 134: 1269–1278.
- Utsui, K., D. Pistillo, and P. Simpson, 2004 Mutual exclusion of sensory bristles and tendons on the notum of dipteran flies. *Curr. Biol.* 14: 1047–1055.
- Verdier, V., J. E. Johndrow, M. Betson, G. C. Chen, D. A. Hughes *et al.*, 2006 *Drosophila* Rho-kinase (DRok) is required for tissue morphogenesis in diverse compartments of the egg chamber during oogenesis. *Dev. Biol.* 297: 417–432.



- Volk, T., and K. VijayRaghavan, 1994 A central role for epidermal segment border cells in the induction of muscle patterning in the *Drosophila* embryo. *Development* 120: 59–70.
- Volohonsky, G., G. Edenfeld, C. Klambt, and T. Volk, 2007 Muscle-dependent maturation of tendon cells is induced by post-transcriptional regulation of stripeA. *Development* 134: 347–356.
- Wayburn, B., and T. Volk, 2009 LRT, a tendon-specific leucine-rich repeat protein, promotes muscle-tendon targeting through its interaction with Robo. *Development* 136: 3607–3615.
- Weitkunat, M., and F. Schnorrer, 2014 A guide to study *Drosophila* muscle biology. *Methods* 68: 2–14.
- Weitkunat, M., A. Kaya-Copur, S. W. Grill, and F. Schnorrer, 2014 Tension and force-resistant attachment are essential for myofibrillogenesis in *Drosophila* flight muscle. *Curr. Biol.* 24: 705–716.
- Winter, C. G., B. Wang, A. Ballew, A. Royou, R. Karess *et al.*, 2001 *Drosophila* rho-associated kinase (Drok) links frizzled-mediated planar cell polarity signaling to the actin cytoskeleton. *Cell* 105: 81–91.
- Xu, B., G. Song, Y. Ju, X. Li, Y. Song *et al.*, 2012 RhoA/ROCK, cytoskeletal dynamics, and focal adhesion kinase are required for mechanical stretch-induced tenogenic differentiation of human mesenchymal stem cells. *J. Cell. Physiol.* 227: 2722–2729.
- Xu, T., and G. M. Rubin, 1993 Analysis of genetic mosaics in developing and adult *Drosophila* tissues. *Development* 117: 1223–1237.
- Zeitlinger, J., and D. Bohmann, 1999 Thorax closure in *Drosophila*: involvement of Fos and the JNK pathway. *Development* 126: 3947–3956.
- Zhang, L., and R. E. t. Ward, 2011 Distinct tissue distributions and subcellular localizations of differently phosphorylated forms of the myosin regulatory light chain in *Drosophila*. *Gene Expr. Patterns* 11: 93–104.

*Communicating editor: I. K. Hariharan*

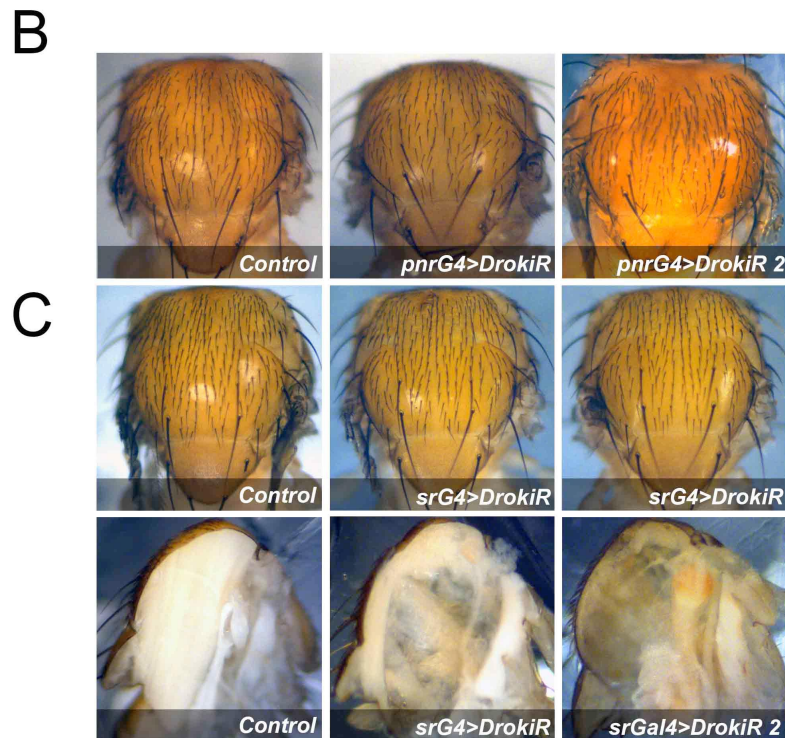
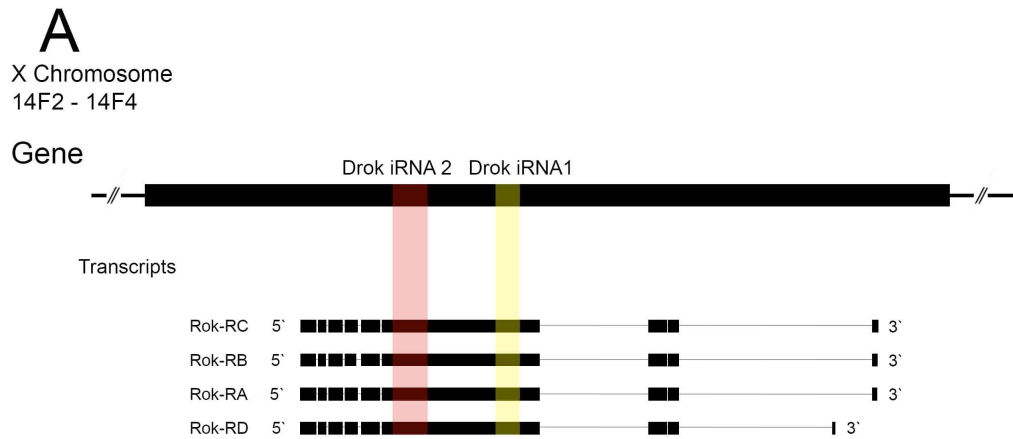


**Figure S1. Two nonF overlapping dsRNA against *Drok* generate similar phenotypes.**

(A) The *Drok* locus (black box) on the X chromosome (at location 14F2-14F4), with transcripts and the dsRNAs used in this study. Red (*Drok dsRNA 2*) and yellow (DrokiR) boxes highlight the regions targeted by the *Drok* dsRNAs. (B-C) Adult notum of flies expressing both *Drok dsRNAi* under the control of *pnrG4* and *srGal4*, with his corresponding sagittal sections of thorax showing DLMs. Note that *DrokiR*



and *DrokiR2* flies display the same phenotype, indicating that our dsRNAs are specific for *Drok*.

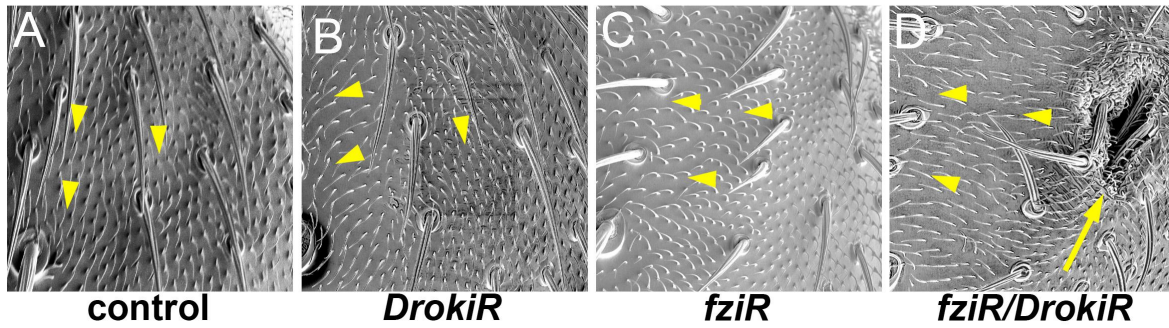


**Figure S2. Double knockdown of *fz* and *Drok* results in invaginations of the notum epithelium at the lateral domains.**

SEM images of adult flies showing orientation of trichomes (arrowheads) and invaginations of the notum epithelium (arrows). Genotypes are indicated below.



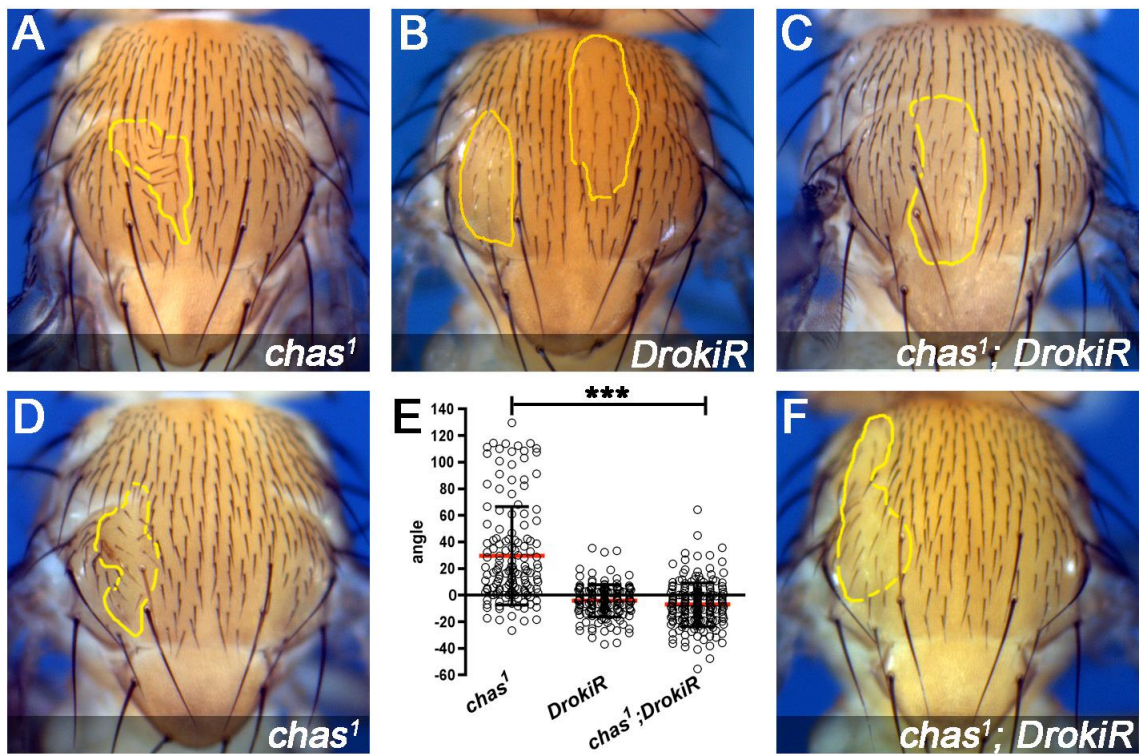


**Figure S3. *Drok* knockdown rescues *chas* LOF phenotypes.**

(A,D) Medial (A) and lateral (D) *chas*<sup>1</sup> clones labeled with *y* display bristles pointing to the midline (mean +/- SD: 29.56 +/- 36.85°, n=145). (E) Chart showing Quantification of lateral and medial bristle angles. (C,F) Expression of *DrokIR* in *chas*<sup>1</sup> clones reverts the orientation phenotypes in medial (C) and lateral positions (F) (p<0.0001). (B, E) Note that the orientation of *chas*<sup>1</sup>; *DrokIR* (-7.184 +/- 16.39°, n=198) is similar to *DrokIR* (-4.179 +/- 12.12°, n=155).

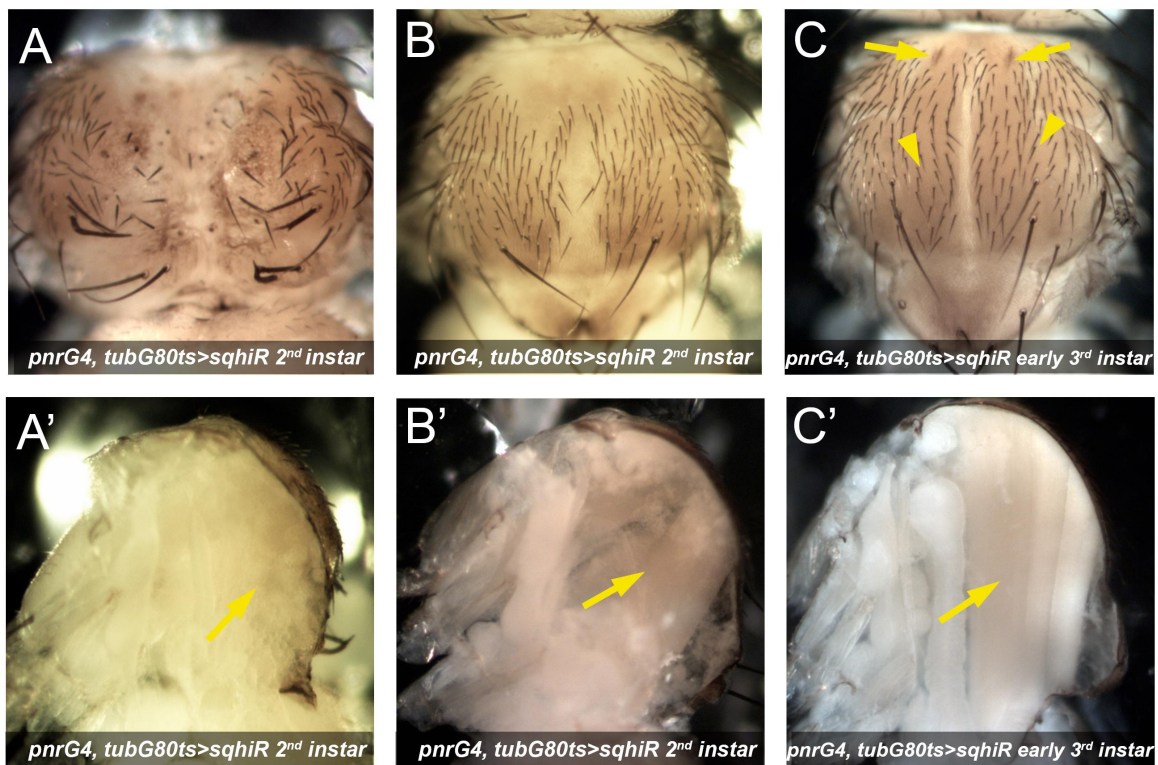


**Figure S4. *Spaghetti squash (sqh)* is required in tendon cells for notum morphogenesis and muscle development.**

(A-B') Expression of *sqhIR* during second instar larval stage results in dorsal thorax closure defects (A-B) and muscle degeneration (A'-B') (arrows). (C-C') Expression of *sqhIR* during third instar larval stage results in invaginations of the epithelium towards anterior (C) (arrows), bristle orientation defects (C) (arrowheads), and does not affect muscle morphology (C') (arrow). (D-F)

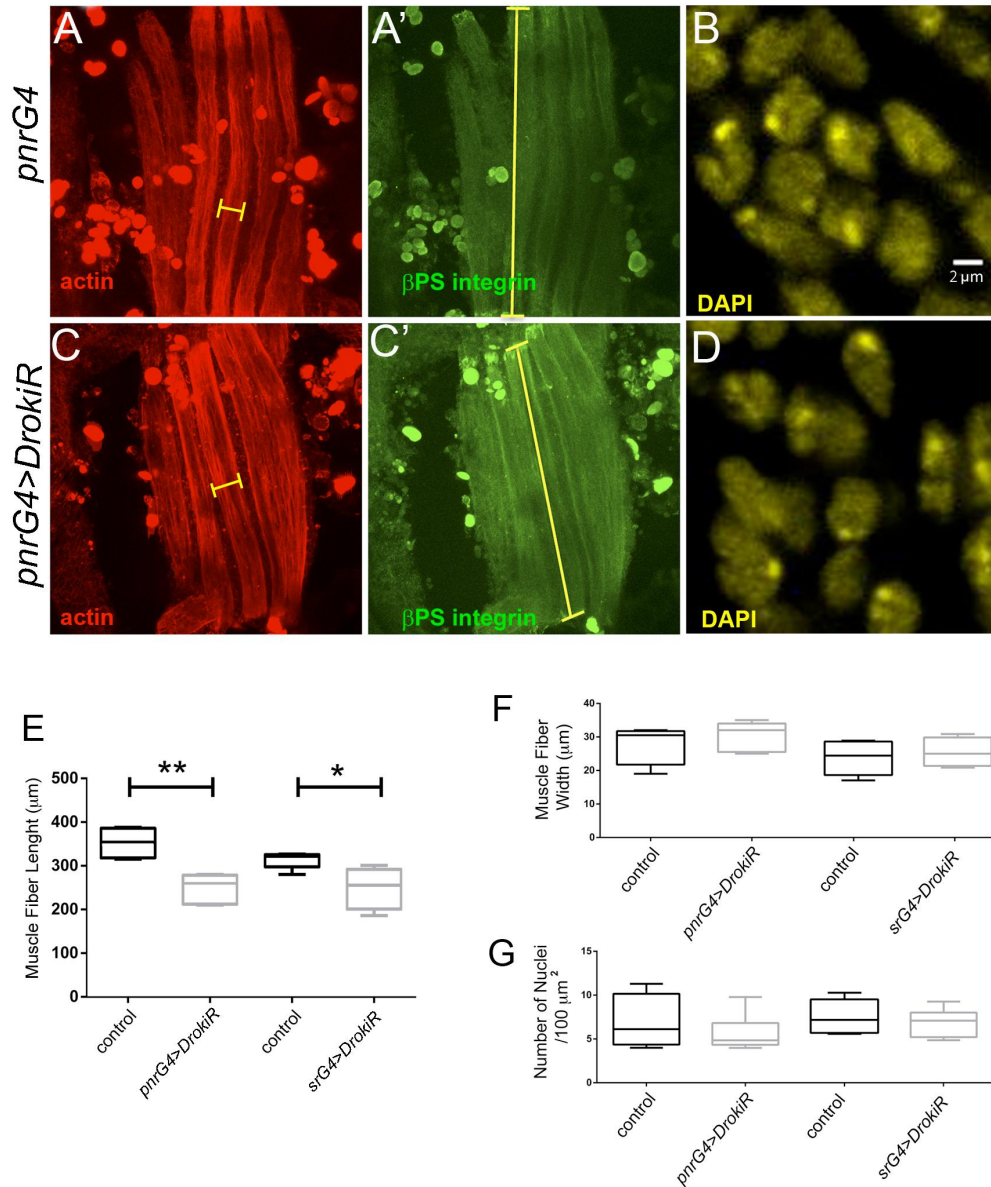


**Figure S5. *Drok* is required in tendon cells for muscle morphogenesis.**

(A, A', C, C') Confocal projections of DLMs stained with Phalloidin/F-actin (A, C), anti  $\beta$ PS-integrin (A',C'). Rulers indicate myotube width (A, C) and length (A',C'). Details of (C) and (C'). (B, D) Nuclei staining with DAPI for quantification. (E-G) Quantification of myotube length (E), width (F) and number of nuclei in 100  $\mu\text{m}^2$  (G).



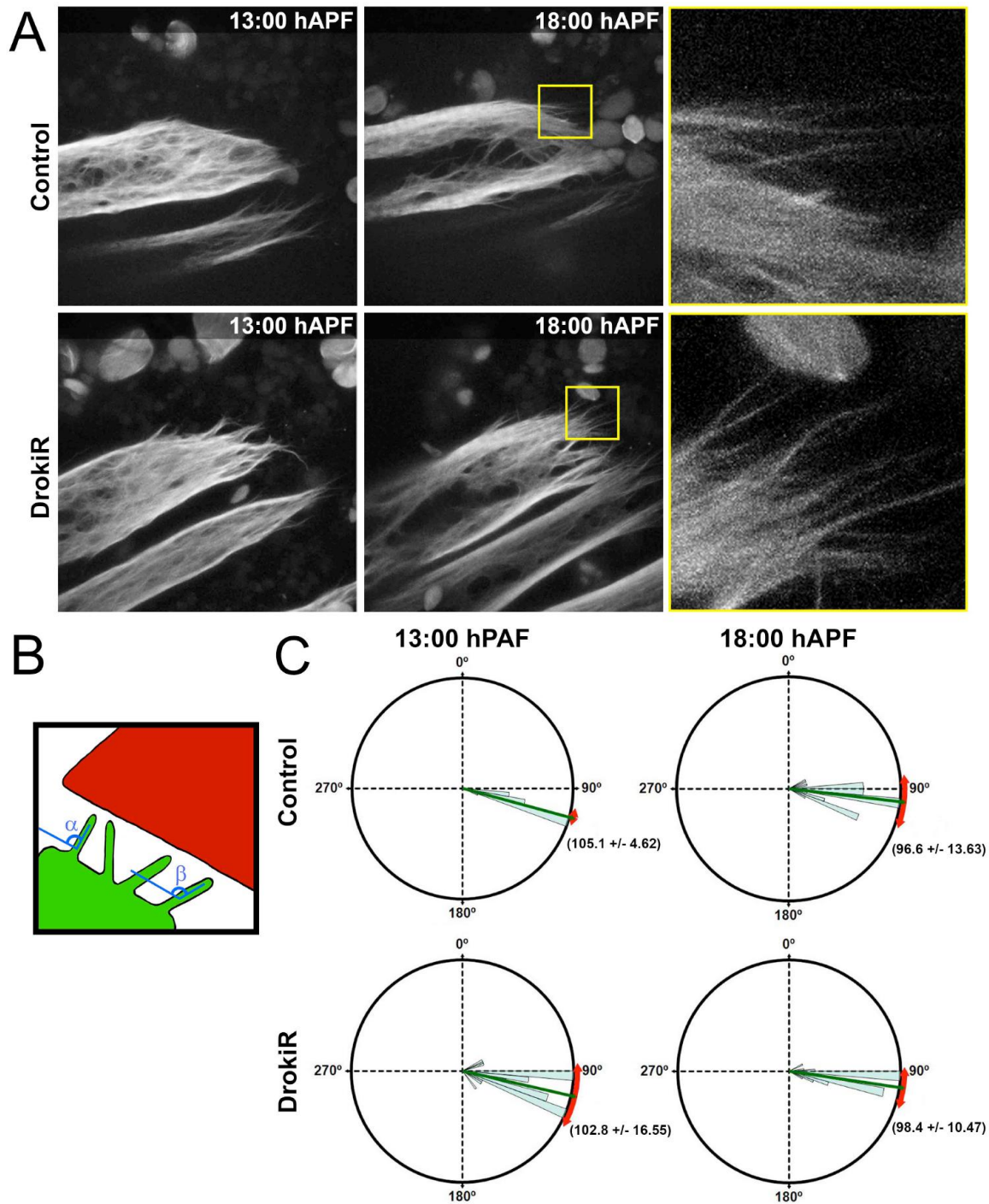


**Figure S6. *Drok* loss of function in tendons cells does not disturb orientation and morphology of muscle filopodia.**

(A) Time points of a time lapse confocal movie taken from 13 to 18 hAPF of flies expressing MHC-TauGFP and CD8RFP driven by *srGal4*. (B) Method to measure the angles formed between muscle processes and the lateral-posterior edge of the *sr* domain. (C) Quantification of muscle extensions angles (13 hAPF  $p < 0.0001$  and 18 hAPF  $p = 0.1887$ ).

**File S2. Drok loss of function does not interfere with dorsal---longitudinal muscle (DLM) migration and attachment initiation.**

Pupa expressing *MHC---tauGFP* to label DLMs and *DrokiR* and CD8---ChRFP under the control of *SrGal4* in tendon cells. Video was recorded starting at ~13 hr APF every 20 min for 5 hr. Movie plays two frames per second. Time is indicated in hour:min. Note that expression of *DrokiR* does not affect muscle migration and attachment initiation. Also note that muscle processes and splitting are not affected. (.avi, 4 MB)

Available for download as a .avi file at:

[www.genetics.org/lookup/suppl/doi:10.1534/genetics.116.189548/-/DC1/FileS2.avi](http://www.genetics.org/lookup/suppl/doi:10.1534/genetics.116.189548/-/DC1/FileS2.avi)

**File S2. Drok loss of function does not interfere with dorsal---longitudinal muscle (DLM) migration and attachment initiation.**

Pupa expressing *MHC---tauGFP* to label DLMs and *DrokiR* and CD8---ChRFP under the control of *SrGal4* in tendon cells. Video was recorded starting at ~13 hr APF every 20 min for 5 hr. Movie plays two frames per second. Time is indicated in hour:min. Note that expression of *DrokiR* does not affect muscle migration and attachment initiation. Also note that muscle processes and splitting are not affected. (.avi, 4 MB)

Available for download as a .avi file at:

[www.genetics.org/lookup/suppl/doi:10.1534/genetics.116.189548/-/DC1/FileS2.avi](http://www.genetics.org/lookup/suppl/doi:10.1534/genetics.116.189548/-/DC1/FileS2.avi)